**Supplementary Figure S1**. Absorbance (◊) and fluorescence (×) of samples generated by a 2× serial dilution of the supernatant from strain Thr-WT. Line of best fit shown for absorbance measurements. Data are the mean of 3 independent replicates, and error bars indicate 1 standard deviation.

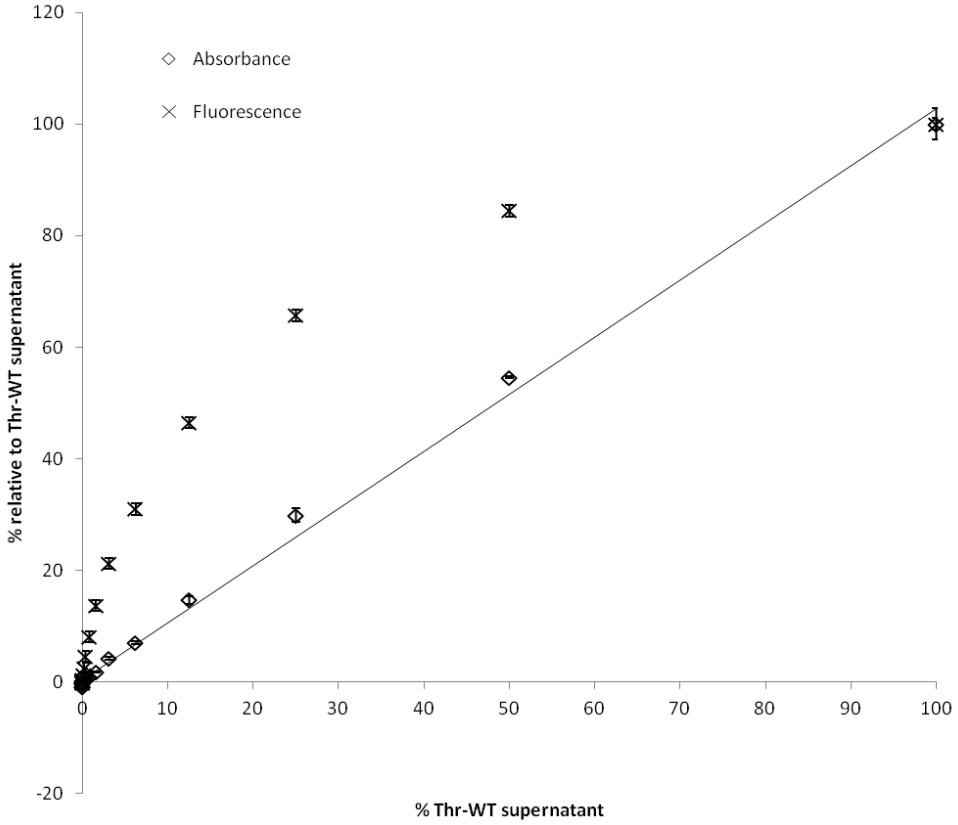

**Supplementary Figure S2**. Mass spectra obtained from the supernatant of the Thr-WT strain, each of the A domain substitution strains, and the *pvdD* deletion mutant (Del). Arrows indicate peaks at 1333.6 m/z, corresponding to wild-type pyoverdine.

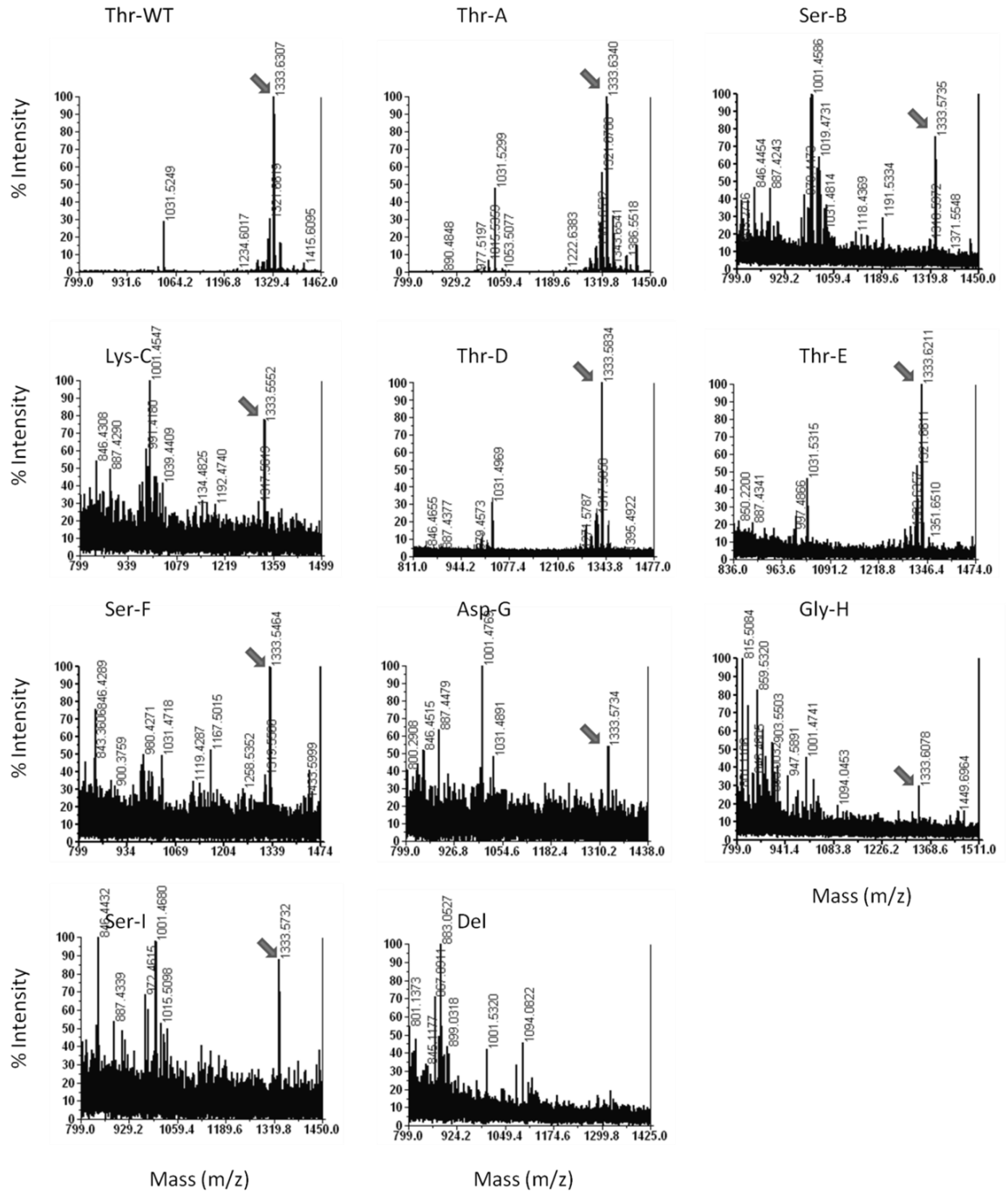

**Supplementary Figure S3.** CID spectra of pyoverdine detected from A domain substitution strains. The five most abundant peaks are indicated by arrows and are annotated in Supplementary Table S3 along with peaks of lower abundance. Peaks labelled by Data Explorer (Applied Biosystems).

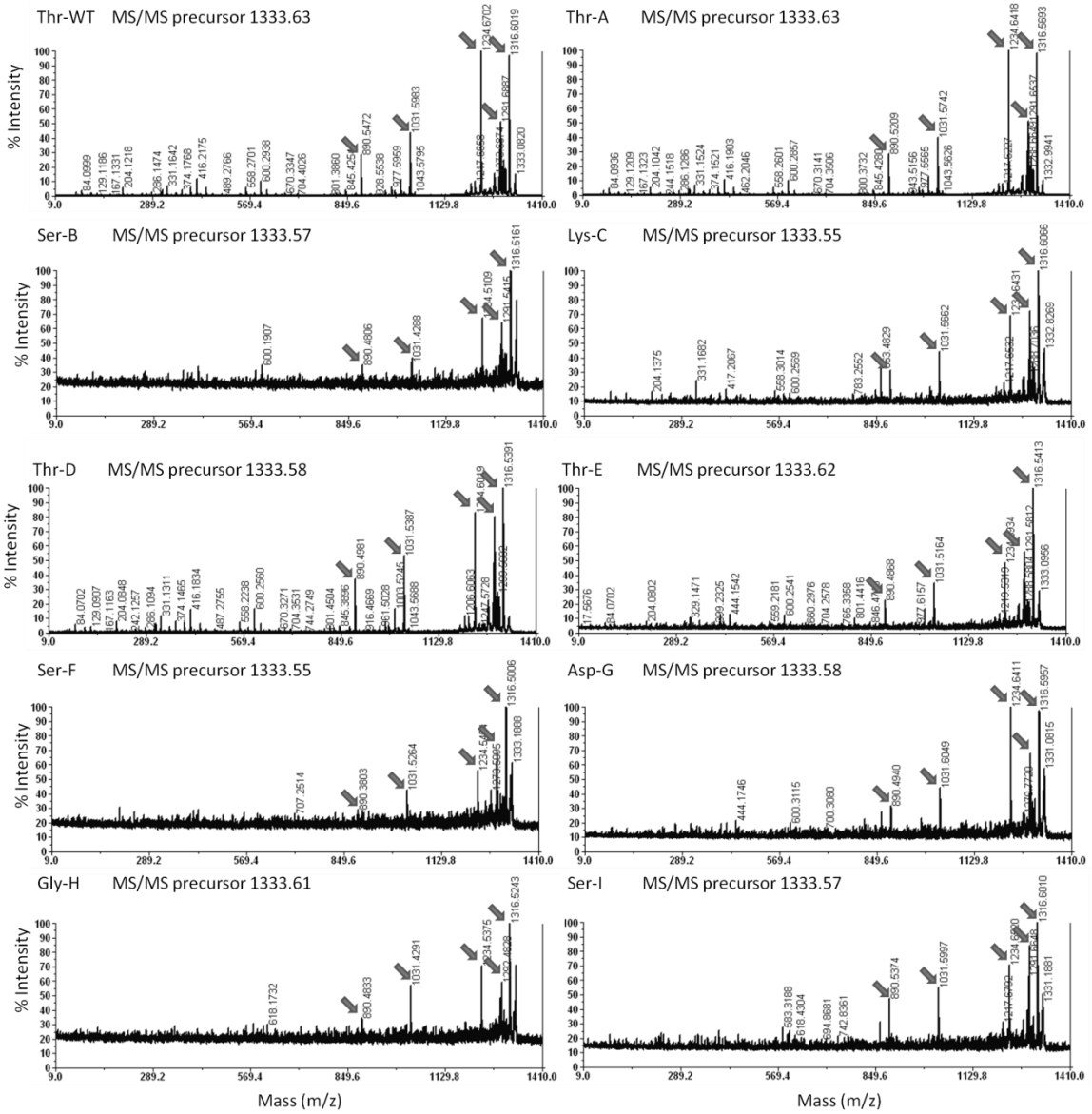

**Supplementary Figure S4**. Mass spectra obtained from the supernatant of the Thr-WT strain, each of the C-A domain substitution strains, and the *pvdD* deletion mutant (Del). Arrows indicate peaks corresponding to the truncated and/or full-length pyoverdine products.

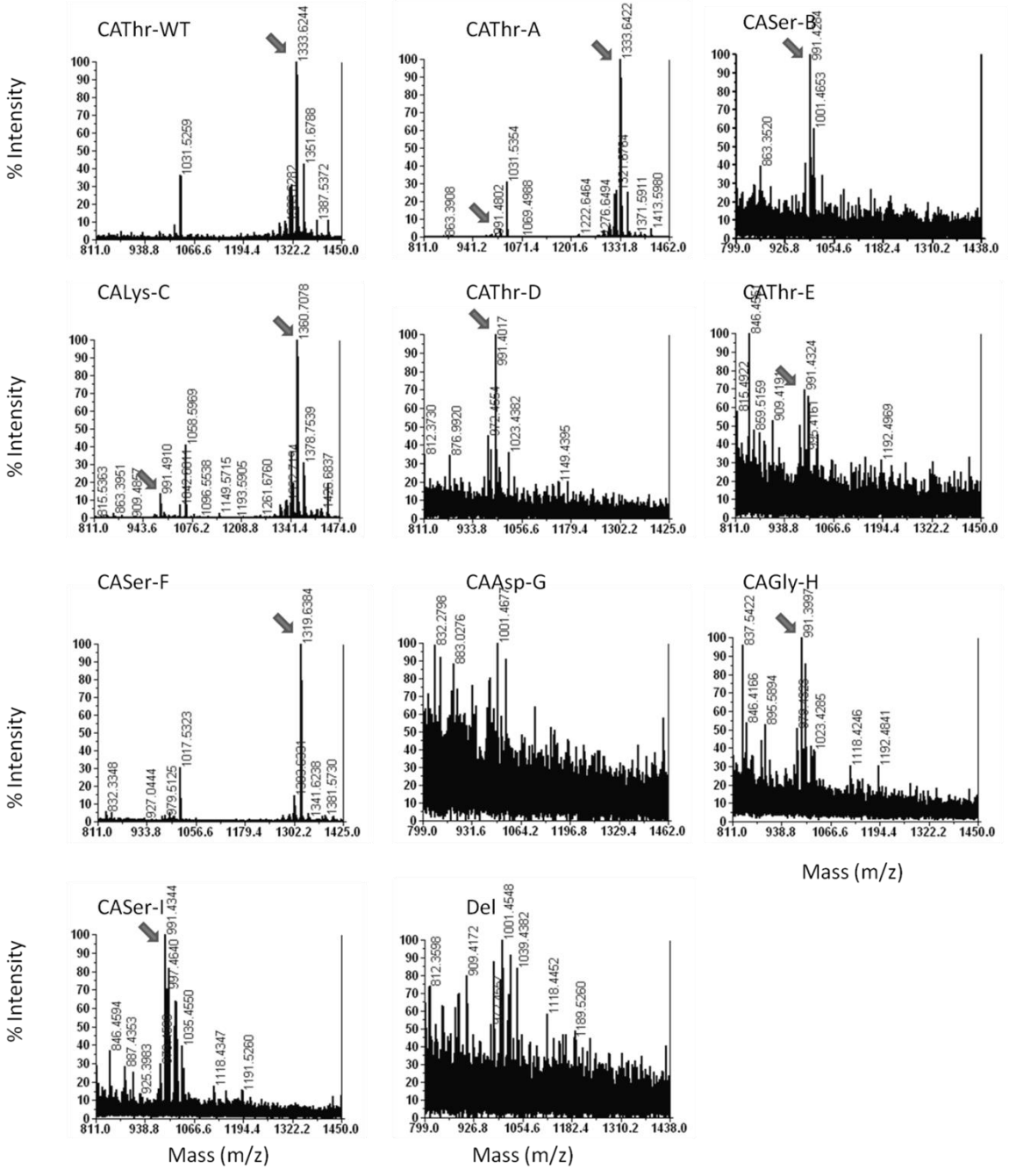

**Supplementary Figure S5**. CID spectra of pyoverdines obtained from C-A domain substitution strains. Arrows indicate abundant ions annotated in Supplementary Tables S4 and S5 that confirm any modifications to the C-terminus of pyoverdine. (A) Spectra of full-length wild-type and modified pyoverdines. (B) Spectra of truncated pyoverdines. Peaks labelled by Data Explorer (Applied Biosystems).

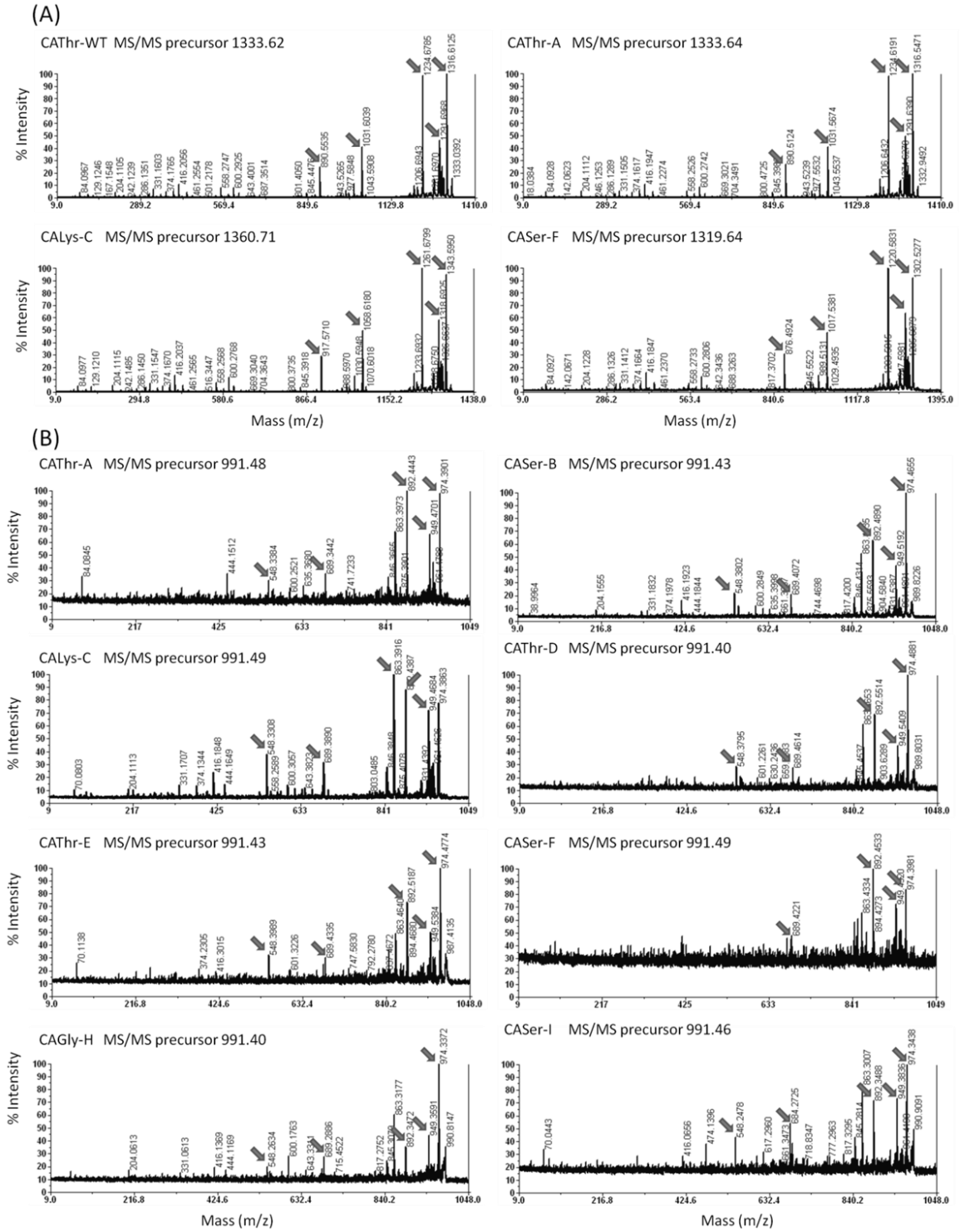

**Supplementary Table S1**. Ions detected by CID of pyoverdine from A domain substitution strains.

| | **Thr-WT** | **Thr-A** | **Ser-B** | **Lys-C** | **Thr-D** | **Thr-E** | **Ser-F** | **Asp-G** | **Gly-H** | **Ser-I** |
|---|---|---|---|---|---|---|---|---|---|---|
| **Ion** | **m/z** | | **m/z** | | | | | | | |
| [RDA + H - Suca]$^+$ | 204.12 | 204.10 | ND | 204.14 | 204.08 | 204.08 | ND | ND | ND | ND |
| $A_1$ - Suca | 317.20 | 317.18 | ND | ND | 317.18 | ND | ND | ND | ND | ND |
| $A_1$ - $NH_3$ | 399.22 | 399.21 | ND | ND | 399.19 | 399.23 | ND | ND | ND | ND |
| $A_1$ | 416.22 | 416.19 | ND | ND | 416.18 | 416.21 | ND | 416.19 | ND | ND |
| $B_1$ | 444.19 | 444.17 | ND | ND | 444.16 | 444.15 | ND | 444.17 | ND | ND |
| $B_2$ | 600.29 | 600.29 | 600.19 | 600.26 | 600.26 | 600.25 | ND | 600.31 | ND | ND |
| $B_3$ | 687.33 | 687.31 | ND | ND | 687.35 | ND | ND | ND | ND | ND |
| $B_4$ | 845.43 | 845.43 | ND | ND | 845.39 | 845.41 | ND | ND | ND | ND |
| $Y_7''$ | 890.55 | 890.52 | 890.48 | 890.53 | 890.50 | 890.49 | 890.38 | 890.49 | 890.48 | 890.54 |
| [RDAb + H]$^+$ | 1031.60 | 1031.57 | 1031.43 | 1031.57 | 1031.54 | 1031.52 | 1031.53 | 1031.60 | 1031.43 | 1031.60 |
| [M + H - Suca]$^+$ | 1234.67 | 1234.64 | 1234.51 | 1234.64 | 1234.60 | 1234.59 | 1234.55 | 1234.64 | 1234.54 | 1234.65 |
| [M + H - $CH_2N_2$]$^+$ | 1291.69 | 1291.65 | 1291.54 | 1291.67 | 1291.60 | 1291.58 | 1291.55 | 1291.66 | 1291.59 | 1291.66 |
| [M + H - $NH_3$]$^+$ | 1316.60 | 1316.57 | 1316.52 | 1316.61 | 1316.54 | 1316.54 | 1316.50 | 1316.60 | 1316.52 | 1316.60 |
| MS/MS precursor | 1333.63 | 1333.63 | 1333.57 | 1333.55 | 1333.58 | 1333.62 | 1333.55 | 1333.58 | 1333.61 | 1333.57 |

Shaded cells indicate ions expected to contain the residue added by the second module of PvdD. Peaks were annotated by comparison to other studies (1–5). Suca, succinamide; RDA, chromophoric fragment from the RDA process; RDAb, peptide chain fragment released by the RDA process; ND, not detected.

**Supplementary Table S2**. Ions detected by CID of major pyoverdine species produced from highly fluorescent C-A domain substitution strains.

| | **Thr-WT** | **Thr-A** | **Lys-C** | **Ser-F** |
|---|---|---|---|---|
| **Ion** | **m/z** | | | |
| $[RDA + H - Suca]^+$ | 204.11 | 204.11 | 204.11 | 204.12 |
| $A_1$ - Suca | 317.19 | 317.18 | 317.18 | 317.16 |
| $A_1$ - $NH_3$ | 399.22 | 399.21 | 399.21 | 399.21 |
| $A_1$ | 416.21 | 416.19 | 416.20 | 416.18 |
| $B_1$ | 444.19 | 444.18 | 444.19 | 444.17 |
| $B_2$ | 600.29 | 600.27 | 600.28 | 600.28 |
| $B_3$ | 687.35 | 687.33 | 687.32 | 687.27 |
| $B_4$ | 845.45 | 845.40 | 845.39 | 845.36 |
| $Y_7''$ | 890.55 | 890.51 | 917.57 | 876.49 |
| $[RDAb + H]^+$ | 1031.60 | 1031.57 | 1058.62 | 1017.54 |
| $[M + H - Suca]^+$ | 1234.68 | 1234.62 | 1261.68 | 1220.58 |
| $[M + H - CH_2N_2]^+$ | 1291.70 | 1291.64 | 1318.69 | 1277.61 |
| $[M + H - NH_3]^+$ | 1316.61 | 1316.55 | 1343.59 | 1302.53 |
| MS/MS precursor | 1333.62 | 1333.64 | 1360.71 | 1319.64 |

Shaded cells indicate ions expected to contain the residue added by the second module of PvdD. Peaks were annotated by comparison to other studies (2–6). Suca, succinamide; RDA, chromophoric fragment from the RDA process; RDAb, peptide chain fragment released by the RDA process; ND, not detected

**Supplementary Table S3**. CID of truncated pyoverdine produced by C-A domain substitution strains.

| | **Thr-A** | **Ser-B** | **Lys-C** | **Thr-D** | **Thr-E** | **Ser-F** | **Asp-G*** | **Gly-H** | **Ser-I** |
|---|---|---|---|---|---|---|---|---|---|
| **Ion** | **m/z** | | | | | | | | |
| [RDA + H - Suca]$^+$ | ND | 204.16 | 204.11 | ND | ND | ND | | 204.06 | ND |
| $A_1$ - Suca | ND | 317.20 | ND | ND | ND | ND | | ND | ND |
| $A_1$ - $NH_3$ | ND | 399.30 | ND | ND | ND | ND | | ND | ND |
| $A_1$ | ND | 416.19 | 416.18 | 416.23 | 416.30 | ND | | 416.14 | 416.07 |
| $B_1$ | 444.15 | 444.18 | 444.16 | ND | ND | ND | | 444.12 | ND |
| $B_2$ | 600.25 | 600.28 | 600.31 | 600.41 | ND | ND | | 600.18 | 600.24 |
| $B_3$ | ND | ND | 687.34 | ND | ND | 687.10 | | ND | 687.29 |
| $B_4$ | 845.43 | 845.41 | 845.38 | 845.45 | ND | ND | | 845.31 | 845.28 |
| $Y_7''$ | 548.34 | 548.38 | 548.33 | 548.38 | 548.40 | ND | | 548.26 | 548.25 |
| [RDAb + H]$^+$ | 689.34 | 689.41 | 689.39 | 689.46 | 689.43 | 689.42 | | 689.29 | 689.27 |
| [M + H - Suca]$^+$ | 892.44 | 892.49 | 892.44 | 892.55 | 892.52 | 892.45 | | 892.35 | 892.35 |
| [M + H - $CH_2N_2$]$^+$ | 949.47 | 949.52 | 949.47 | 949.54 | 949.54 | 949.45 | | 949.36 | 949.38 |
| [M + H - $NH_3$]$^+$ | 974.39 | 974.47 | 974.39 | 974.49 | 974.48 | 974.40 | | 974.34 | 974.34 |
| MS/MS precursor | 991.48 | 991.43 | 991.49 | 991.40 | 991.43 | 991.49 | ND | 991.40 | 991.46 |

Shaded cells indicate ions reduced in m/z corresponding to loss of the three terminal pyoverdine residues. Peaks were annotated by comparison to other studies (2–6). Suca, succinamide; RDA, chromophoric fragment from the RDA process; RDAb, peptide chain fragment released by the RDA process; ND, not detected.

*Cells for ions detected by CID are empty due to corresponding precursor ion remaining undetected.

**References for Supplementary Material**


1. **Budzikiewicz H, Schäfer M, Fernández DU, Matthijs S, Cornelis P**. 2007. Characterization of the chromophores of pyoverdins and related siderophores by electrospray tandem mass spectrometry. Biometals **20**:135–144.
2. **Demange P, Wendenbaum S, Linget C, Mertz C, Cung MT, Dell A, Abdallah MA**. 1990. Bacterial siderophores: structure and NMR assignment of pyoverdins Pa, siderophores of *Pseudomonas aeruginosa* ATCC 15692. Biometals **3**:155–170.
3. **Fuchs R, Budzikiewicz H**. 2000. Structural studies of pyoverdins with cyclopeptidic substructures by electrospray ionization and collision induced fragmentation. J. Spectroscopy **14**:229–246.
4. **Hannauer M, Schäfer M, Hoegy F, Gizzi P, Wehrung P, Mislin GLA, Budzikiewicz H, Schalk IJ**. 2012. Biosynthesis of the pyoverdine siderophore of P*seudomonas aeruginosa* involves precursors with a myristic or a myristoleic acid chain. FEBS Lett. **586**:96–101.
5. **Mossialos D, Ochsner U, Baysse C, Chablain P, Pirnay J-P, Koedam N, Budzikiewicz H, Fernández DU, Schäfer M, Ravel J, Cornelis P**. 2002. Identification of new, conserved, non-ribosomal peptide synthetases from fluorescent pseudomonads involved in the biosynthesis of the siderophore pyoverdine. Mol. Microbiol. **45**:1673–1685.